

# In-situ Versatile Characterization of Carbon NanoTubes using Nanorobotics

Cédric Clévy<sup>1</sup>, Bruno Sauvet<sup>1</sup>, Jean-Yves Rauch<sup>1</sup>, Olivier Lehmann<sup>1</sup>, François Marionnet<sup>1</sup>, Philippe Lutz<sup>1</sup>, Lorenzo Beccacece<sup>2</sup>, Stéphane Xavier<sup>2</sup>, Raphael Aubry<sup>2</sup>, Afshin Ziaei<sup>2</sup>, Claude Prévot<sup>2</sup>, Guillaume J. Laurent<sup>1</sup>

**Abstract**—The paper investigates electrical characterizations of CNTs (carbon nanotubes) within a SEM chamber. The originality of the proposed approach relies in its high versatility that is made possible thanks to nanoprobe moved by 6-DoF nanopositioning robots. Using this configuration, the influence of several factors are evaluated to know the electrical behavior of the measurement system. The paper presents several experimental characterizations of CNTs. The measured values of electrical resistance are in complete agreement with known results from the literature but were obtained in a much more versatile way.

## I. INTRODUCTION

Nanotechnologies is a fastly growing field from both industrial and scientific point of views. The recent emergence of many innovative materials and nano-objects with outstanding characteristics goes with the need to study them and also to combine them to form more complex arrangements such as Nano-Electro-Mechanical-Systems (NEMS), nano-sensors or nano-optical devices. Among all existing applications, a specific interest is paid to Carbon NanoTubes (CNTs) because they highlight particularly promising performances and are expected to revolutionize many applications (nanoelectronics, sensing, thermal conduction, medical field, computers). Also, many kinds of CNTs, or structures based on CNTs, can now be obtained by various ways and there are pressing needs to characterize their performances and to identify some key parameters (mechanical, electrical, field emission, chemical, optical, thermal). For this reason, new investigations especially on both developing new tools and new protocols are required. Experimental characterizations of CNTs mainly rely on devices specifically designed for their measurement that successfully enabled to achieve deeper analysis and quantification of several key parameters [1]. Developing new tools and methods that could enable to obtain these kinds of result in a much more versatile and in-situ SEM clearly appears.

To target this objective, among all existing characterization to manufacturing techniques (self-assembly, chemical synthesis, electron beam lithography, mobile nanoparticles...), the use of nanorobotic platforms recently demonstrated extremely high interest through achieving, in an original way, nanomanipulation and nano-assembly tasks offering

disruptive characterization and nanomanufacturing potential [2]. These works conducted to notable achievements such as: characterization of nanowires [3] [4], graphene membranes [5], assembly of photonic crystal device [6], nano-wire based transistors [7], detailed study of DNA [8], understanding neuronal connections [9] and many others. Robotized and sometimes automated tasks mainly concern nanowires manipulation or nanoprobe but demonstrated high interest over other techniques: experiments are done faster (minimization of drift phenomena, throughput increase), in a more repeatable way but also with much high versatility meaning the experimental platform can be easily reconfigured or adapted to different kinds of experimentations [10] [11] [12] [13] [14].

Thus, the goal of this paper is to show high accurate electrical measurements on CNTs, in-situ SEM and in a versatile way through nanorobotic tools and methods. For that, section II introduces the experimental platform and developed approach. Section III highlights the reference electrical behavior of the experimental measurement system while section IV is focused on measurements done on vertically grown CNTs using nanotips.

## II. THE EXPERIMENTAL PLATFORM

To investigate the versatile experimental characterization of CNTs through a nanorobotics approach, a nanorobotic platform has been integrated inside of the room chamber of a SEM. The platform comprises several robots carrying very thin probes that are connected with an electronic circuit enabling the measurement of very small electrical currents. These systems are presented in details below.

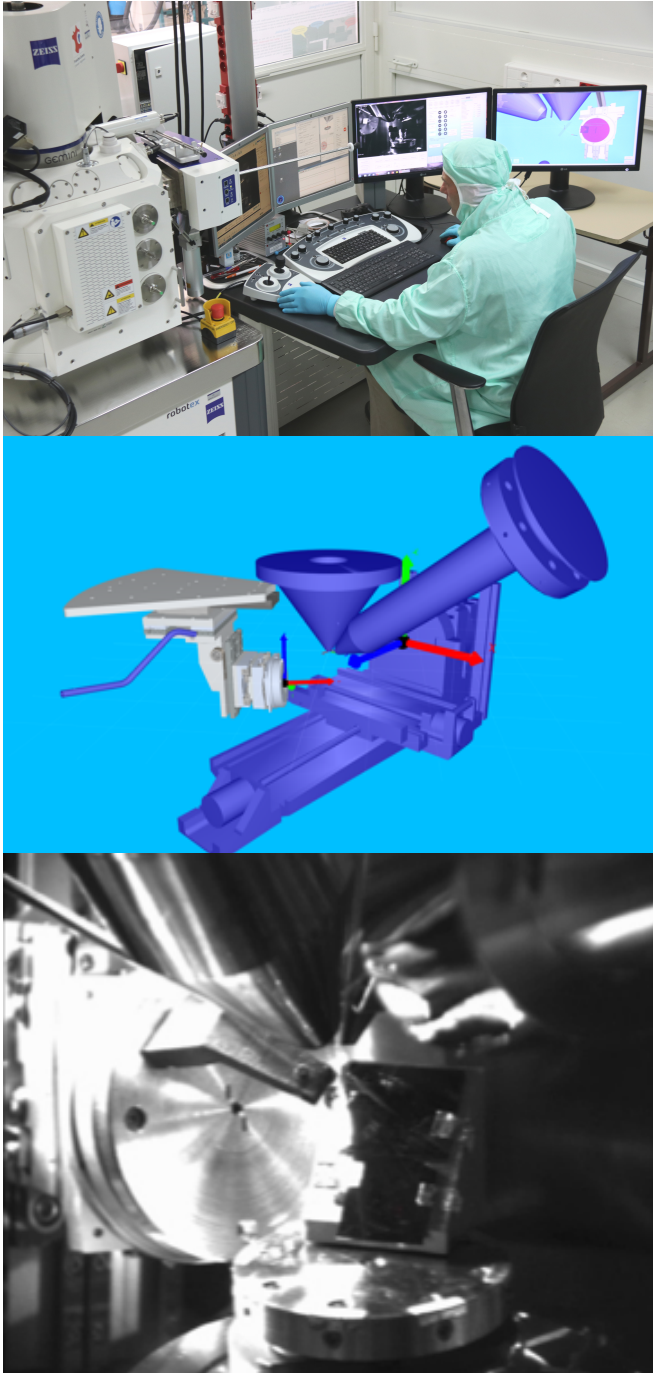
### A. Nanorobotic platform in-situ SEM

The experimental platform used is the  $\mu$ Robotex platform (Fig. 1) that already demonstrated impact-full achievements such as the assembly of a house at the tip of an optical fiber [2] or by the assembly of nanophotonics components in a dynamic way with a positioning accuracy of some tens of nanometers [15]. It is based on a Zeiss AURIGA 60 Cross-Beam Scanning Electron Microscope (SEM), combining an electron gun, a Gallium ion gun and a gas injector. Inside the chamber of this electron microscope, in addition to the standard 6-axis 5-DoF stage, a 6-axis 6-DoF robot and a 3-axis robot have been added.

The 5-DoF stage allows the pre-positioning of the elements to be handled and assembled, it is used as a first hand.

<sup>1</sup> FEMTO-ST institute, Univ. Bourgogne Franche-Comté, CNRS, AS2M département, 24 rue Savary, 25000 Besançon, France cclevy, jyves.rauch, olivier.lehmann, guillaume.laurent@femto-st.fr

<sup>2</sup> Thales Research and Technology, F-91767, Palaiseau, France



**Fig. 1:** The  $\mu$ ROBOTEX platform used for these works: the SEM-FIB-GIS can be seen on the top image while the HMI interface including the virtual representation of the inside part of the platform chamber can respectively be seen on the middle and bottom images.

It has little dexterity, as it is usually used to position samples for imaging. The actuators are stepper motors. The 6-DoF robot is used as the second hand of the platform. Allowing easy positioning under both beams, it has a positioning resolution of few nanometers and much higher motion generation capacities thanks to the robotic control of this system. The actuators are stick-slip types and are closed loop controlled. The 3-axis robot operates in an open loop allowing a third hand in case of need for temporary holding of objects or in the context of future development to position specific tools as close as possible. The actuators are also stick-slip kinds that enables a positioning resolution of few nanometers.

### B. HMI for dexterous and accurate robotic tasks

All these elements are controlled via an Human-Machine-Interface (HMI) that allows:

- to dialog with the human operator(s) around the platform, via (1) a three-dimensional virtual representation of the internal elements of the chamber, and (2) a graphical interface allowing to control both main hands,
- to control the axis of the 5-DoF stage and of the 3-axis robot,
- to control and synchronize in real time, the motions of the 6-DoF robot.

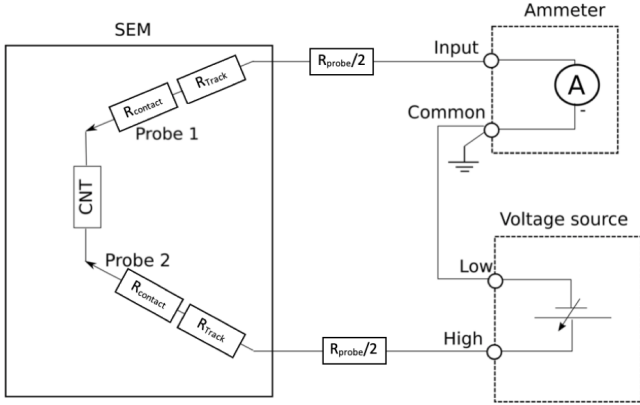
The system controlling the 6-DoF robot uses a real-time system clocked at 2kHz, based on a Twincat 3.1 system provided by Beckhoff. The control of the drives of the robot axis is carried out via the generation of "pulse+dir" signals. All I/O are connected via an Ethercat bus, ensuring very accurate synchronization. Finally, the axis drives are configured via an RS232 connection. The configuration parameters concerned here are mainly the step lengths controlled by the "pulse+dir" signals. The robot's movements are generated thanks to:

- a speed profile calculated by the real-time system based on a digital filter that integrates the jerk into each cycle into acceleration and then speed. This allows a continuous profile in speed and acceleration, avoiding sudden changes.
- the generation of joint movements using these profiles.
- the generation of cartesian movements using these profiles as well as the kinematic model of the robot. This kinematic model uses the modified Khalil-Kleininger representation [16]. Its parameters have been calculated by an in-situ calibration procedure to achieve the most accurate movements.

As the geometry of the entire chamber is known, frames are associated with both beams to allow easy movements in the images, it is then possible to build, as for large-scale robots, any tool center points (TCP) necessary for manipulations or assemblies.

### C. Low current measurement based on nanoprobing

Using the above presented nanorobotics and HMI, two nanoprobes are used and handled by robot hands 2 and 3 to enable their motion. These probes have very thin tip (radius of 5nm) and can then establish a mechanical contact



**Fig. 2:** Principle scheme of the electrical circuit used including a pico-ammeter, two probes and a CNT placed inside of the vacuum chamber of the SEM.

between one probe and a vertically growth CNT. Both probes are included in an electrical circuit that also includes a pico-ammeter KEYSIGHT TECHNOLOGIES AI-B2987A 2). Using this approach, it is then possible to achieve many kinds of measurements in a versatile way by contacting the two probes along one same CNT (to measure its electrical characteristics) or between a CNT and its embedding (characteristics of the electrical contact) or to manipulate several CNT (measurement of their electric contact).

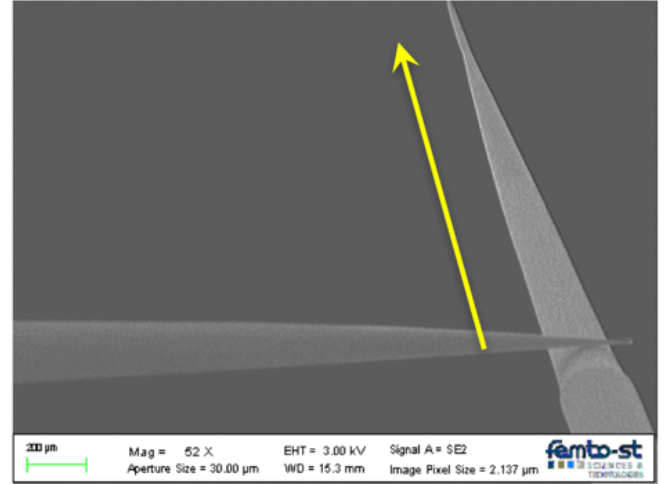
### III. ELECTRICAL BEHAVIOR OF THE MEASUREMENT SYSTEM

Before starting to achieve measurements of CNTs, reference measurements have been achieved in order to establish the electrical behavior of the measuring system including pico-ammeter, probes, cabling, feedthrough but also to consider the basic influence of the environments (air and vacuum) onto the measurement itself.

#### A. Influence of the contact between probes

First experiments have been done consisting in establishing a mechanical contact between the two probes. It has been noticed that the way the contact appears influences the electrical measurements. An experiment has been done starting by establishing a contact between the very tip of one probe (5 nm radius) with a more rigid part (where the cross section is about  $40 \mu\text{m}$  in diameter) of the second one as displayed on Fig. 3. Once this first contact established, and thanks to the highly accurate nanorobot trajectory control, the tip of the first probe was sliding along the second one up to tip-tip contact (yellow arrow on the Figure).

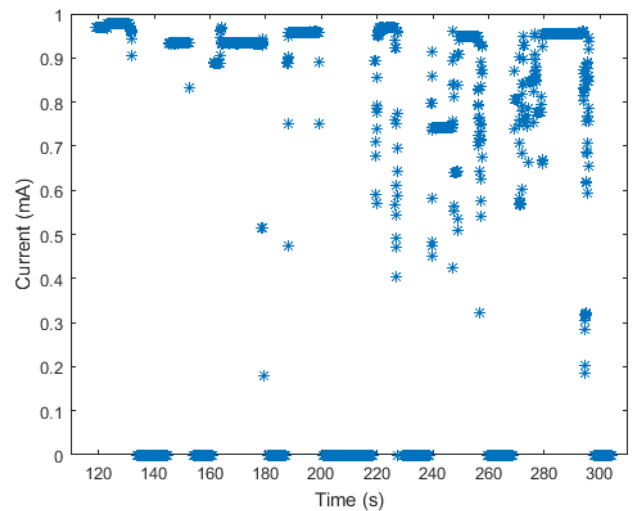
During this motion, the corresponding current was measured. Related experimental result is shown in Fig. 4. The initial contact is created at time  $t = 120$  s, after which the first tip slides along the second one. During this sliding, the electrical contact does not remain constant, small jumps appears. Nevertheless, the maximum current measured always remains close to 1 mA. Considering that the supply voltage



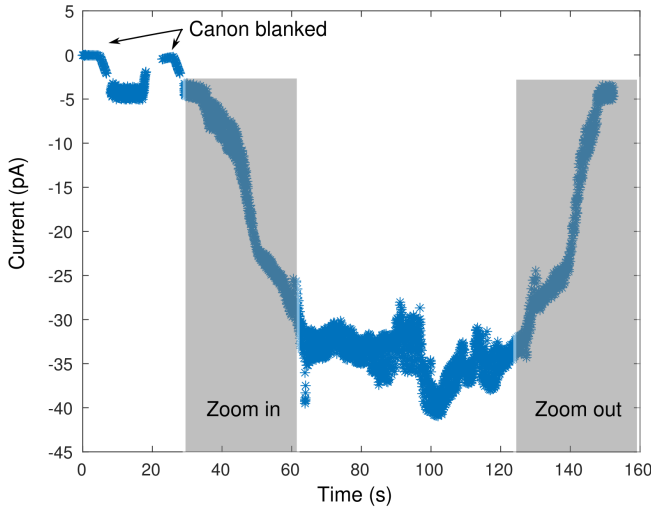
**Fig. 3:** Image of the initial contact between two tips followed by a sliding motions between them following the yellow arrow.

is 0.01 V, the average resistance for the electric circuit based on tip-tip contact between the probes is  $2R_{\text{probe}} = 10 \Omega$ .

The curve also highlights that the starting of the curve shows sudden jumps between null and 1 mA level while going forward along tip-tip contact induces less strict jumps. Jumps are likely induced by motions and small mechanical related jumps inducing temporary loss of electrical contact during the motion. More noisy signal happening for  $t > 220$  s appears due to the quite low stiffness of the probes that is largely reduced when approaching their tip part. One can also note that despite the very low tip diameter (5 nm radius), there is no additional electrical resistance induced by the tip diameter at their extreme end. As a conclusion, electrical measurements using probes with very thin tip can



**Fig. 4:** Evolution of the current crossing the two probes when the left tip follows the yellow arrow. The supply voltage is 0.01 V.



**Fig. 5:** Influence of the Electron Beam onto the current measured. The acceleration voltage is set to 3 kV.

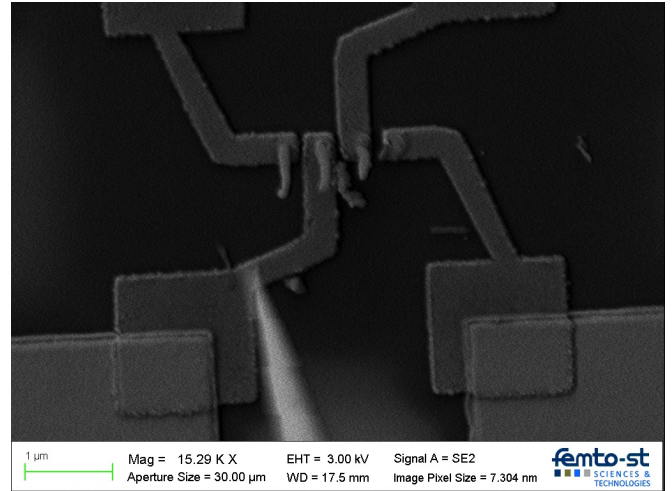
be achieved based on the maximum level of current measured even in the presence of short losses of electrical contact.

In the same way, the resistance of the electric track on the substrate was measured to be  $R_{track} = 344 \Omega$ .

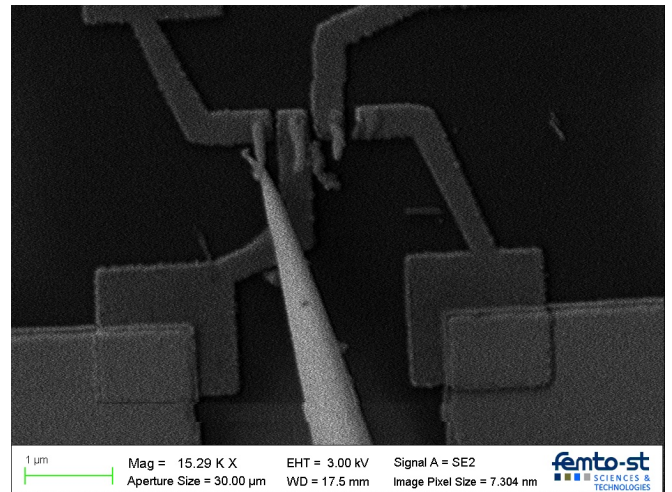
### B. Influence of the SEM environment and measuring conditions

Achieving electrical measurement of CNTs at the same time than achieving visualization of these CNTs can be highly helpful and can clearly help to understand phenomenon. Nevertheless, the vacuum environment of the SEM chamber may influence the measurement. Especially, the electron beam used to visualize the samples may influence the electrical measurements especially because current measured on CNTs may be pretty low.

To quantify the influence of such factors, an experiment has been achieved, the corresponding plot is displayed on Fig. 5. During this experiment, the current collected by the probe is recorded. For  $t < 30$  s, the electron gun emits electrons to visualize the probe. During this time, the electron gun is blanked two times (the electrons are emitted but cannot go in the chamber). When the beam is blanked, no current is measured demonstrating no influence of the blanked beam as expected. When the gun is not blanked, small currents can be measured (about 5 pA). Latter, i.e. when  $30 \text{ s} < t < 80$  s, a zoom in of the SEM image is achieved (from 16x to 12000x) inducing an increased concentration of electrons on the probe. During this time the influence on current measured is demonstrated and reaches 45 pA. Once the zoom is kept constant ( $80 \text{ s} < t < 125$  s), the current measured remains constant meaning the influence of charges induces by the electron beam on the sample. Latter on, i.e. for  $t > 125$  s, a zoom out of the image is achieved, during this time, the current measured reduces reaching at the end the initial level met before the zoom in. This fact highlight, that the dependence between electron beam



**Fig. 6:** Probe tip almost in contact with the CNT.




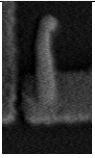
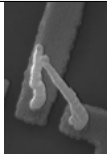
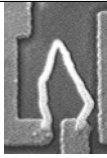
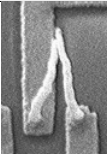
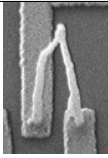

**Fig. 7:** Probe tip in contact with the tip of the CNT.

and current measured are correlated and this phenomenon appears pretty reliable. As a conclusion of this experiment, it is also important to note that the current induced by the electron beam may reach 45 pA which does not appear meaningful when achieving measurement on CNTs (please refer to the following section).

## IV. ELECTRICAL MEASUREMENTS OF VERTICAL CNTS

After reference experiments investigated during the previous section, electrical measurements on CNTs have then been achieved. Two kinds of experiments were performed, the first ones deal with single CNT to probe contact while the second kind of experiments deals with CNT-CNT connected nanodevices. For both configurations, the measurement of electrical resistance appears pretty useful for many applications. Knowing the current measured and the voltage applied, the resistance could be estimated. Also, the resistivity can be estimated by  $\rho = R * S/L$  knowing the length (L), diameter (2xR) and thus the related cross section (S) of the CNT that can be estimated using SEM visualization.



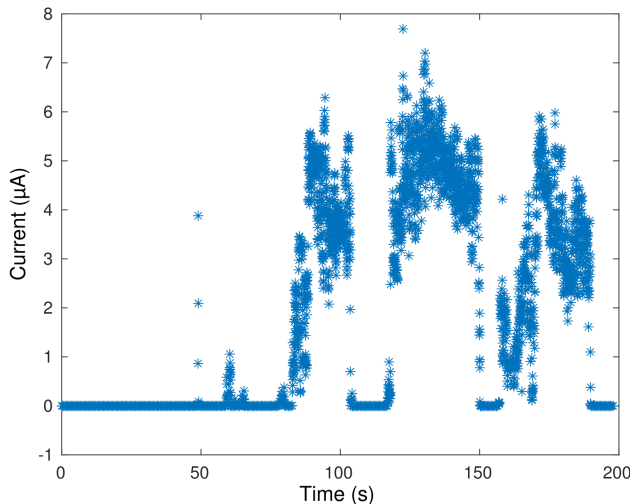
Experiment	CNT-probe measurements			CNT-CNT measurements			
Sample							
	1	2	3	4	5	6	7
Length (nm)	2520	2950	6307	6790	5343	6565	7300
Resistance (kΩ)	12.7	9.1	31.7	30.0	18.4	22.8	18.5

**TABLE I:** Measured resistances and lengths for seven samples.

### A. Single-CNT-probe measurements

The investigated devices consist in CNTs that have grown vertically on a base electrode. During experiments, one probe was placed in contact with the electrode while the second probe was used to touch the tip of the CNT. Fig. 6 shows the typical state of the second probe right before being in contact with the CNT and Fig. 7 shows this same probe once in contact with the CNT, in the highlighted case, the CNT is slightly bent. During this experiment the current is recorded (Fig. 8). As noted in the preliminary experiments (reference measurements), the current does not appear constant due to the bending of the CNT but also to their relative motion during the experiment that may induce some sliding and contact losses. Despite that phenomena, and based on the analysis done in the previous reference measurements, it appears that a current of  $7.7 \mu\text{A}$  is measured for a supply voltage of  $0.1 \text{ V}$ . The related resistance is  $R_1 = 12.7 \text{ k}\Omega$  that corresponds to the sum of resistances of the CNT, of the probes, of the track and of the CNT-track contact such as:

$$R_1 = \rho * L_1/S + 2R_{probe} + R_{track} + R_{contact}$$



**Fig. 8:** Evolution of the current when the probe goes in contact with the tip of a CNT. The supply voltage is  $0.1 \text{ V}$ .

where  $L_1 = 2520 \text{ nm}$  is the length of the CNT (measured in the SEM image) and  $S = \pi D^2/4$  is the cross-section of the CNT (the diameter of CNTs is  $D = 180 \text{ nm}$ ).

A second CNT has been measured in the same way. The measured resistance is  $R_2 = 9.1 \text{ k}\Omega$  for a length of  $L_2 = 2950 \text{ nm}$ .

### B. CNT-CNT measurements

The other experiments that have been done deal with CNT-CNT contacts when both CNTs are already in contact either because they have been fabricated in this way or because they have been manipulated to reach this configuration. The samples and the experimental results are collected in Table 1 together with previous measurements.

Assuming that all the CNTs have approximately the same diameter and that the resistance of the contacts between CNTs and electric tracks are also identical, the resistance of the circuit can be expressed by:

$$R_i = \rho * L_i/S + 2R_{probe} + 2R_{track} + 2R_{contact}$$

### C. Synthesis

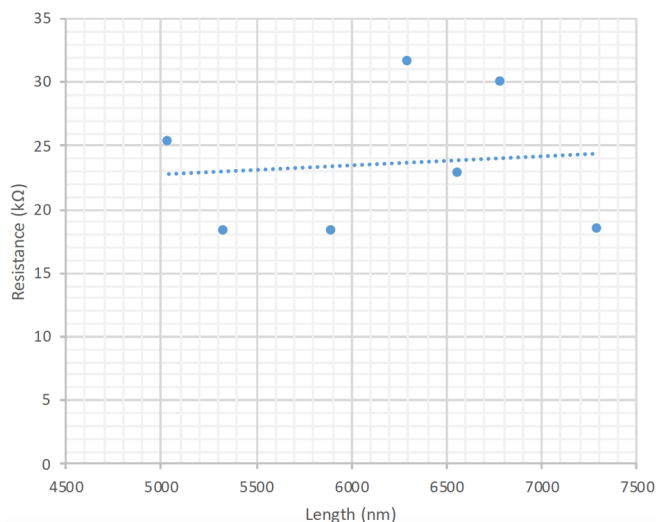
Fig. 9 presents the same results into graphical form. The CNT-probe measurements have been multiplied by two to be represented on the same scales. The line on the graph corresponds to the linear regression of the measured values.

The slope corresponds to the ratio  $\rho/S$  and is equal to  $7.19\text{e}8$  leading to a resistivity of  $1.8 * 10^{-5} \Omega \cdot \text{m}$ . This value appears in very good agreement with previous measurements provided by the state-of-the-art that have been obtained by other techniques such as highlighted by the survey written by Jasulaneca et al. in [1].

The y-intercept of the line is equal to the sum of circuit resistances  $R_{probe} + 2R_{track} + 2R_{contact} = 19.1 \text{ k}\Omega$ . The identified value of the resistance between a CNT and the track is then  $9.2 \text{ k}\Omega$ . This value is very close to  $8.8 \text{ k}\Omega$  which corresponds to the direct measurement of this contact resistance by mechanical removing a CNT and testing its footprint.

## V. CONCLUSION

The pressing need to characterize nanodevices, especially the ones based on CNTs, conducted to propose a versatile approach enabling the electrical characterization of CNTs based on nanorobotics. The approach notably relies on



**Fig. 9:** Measured resistance vs length for the seven samples.

nanoprobe-based nanomanipulation, pico-ammeter for the measurement of weak electrical signals and an adequate experimental procedure to merge versatility and high quality measurements. Works firstly enabled to establish the correlation between electrical measurement and working of the electron gun. Also, the way nanoprobe contact influences electrical measurement has been investigated. Several experimental results on CNTs have also been achieved demonstrating that resistance and resistivity of CNT for both CNT-probe and CNT-CNT contact can be obtained. Numerical values obtained appear to be in very good agreement with the ones provided by the literature but that can be obtained in a much more versatile way (no need of dedicated design and fabrication works). This specific characteristic enables to envision short time, high quality measurements that can be done in-situ SEM meaning that several measurements (electrical and vision for instance) could clearly be coupled.

#### ACKNOWLEDGMENTS

This work was supported by the French "Investissements d'Avenir" program by the project ISITE-BFC (contract ANR-15-IDEX-03) Nanofactory, by the Equipex ROBOTEX (ANR-10-EQPX-44-01) and by the Région Bourgogne Franche-Comté. Authors also acknowledge the French RENATECH network through its FEMTO-ST technological facilities MIMENTO and the EIPHI Graduate School (ANR-17-EURE-0002).

#### REFERENCES

- [1] Jasulaneca, L., Kosmaca, J., Meija, R., Andzane, J., and Erts, D. (2018). Electrostatically actuated nanobeam-based nanoelectromechanical switches—materials solutions and operational conditions. *Beilstein journal of nanotechnology*, 9(1), 271-300.
- [2] Rauch, J. Y., Lehmann, O., Rougeot, P., Abadie, J., Agnus, J., and Suarez, M. A. (2018). Smallest microhouse in the world, assembled on the facet of an optical fiber by origami and welded in the Micro-Robotex nanofactory. *Journal of Vacuum Science and Technology A: Vacuum, Surfaces, and Films*, 36(4), 041601.

- [3] Lugstein A, Steinmair M, Steiger A et al. Anomalous piezoresistance effect in ultrastrained silicon nanowires. *Nano Letters* 2010; 3204–3208., 10
- [4] Zhu Y, Qin Q, Xu F et al. Size effects on elasticity, yielding, and fracture of silver nanowires: In situ experiments. *Physical Review B* 2012; 045443., 85
- [5] Zimmermann S, Tiemerding T, Fatikow S. Automated robotic manipulation of individual colloidal particles using vision-based control. *IEEE/ASME Transactions on Mechatronics* 2015, and 20: 2031–2038. n.d.
- [6] Aoki K et al. (2003) Microassembly of semiconductor three-dimensional photonic crystals. *Nature Materials*,; 117–121., 2:
- [7] Zhang YL, Li J, To S et al. Automated nanomanipulation for nanodevice construction. *Nanotechnology* 2012; 065304., 23:
- [8] Chen BK, Anchel D, Gong Z et al. Nano-dissection and sequencing of DNA at single sub-nuclear structures. *Small* 2014; 3267–3274, 10:
- [9] Xiao L, Michalski N, Kronander E et al. BMP signaling specifies the development of a large and fast CNS synapse. *Nature Neuroscience* 2013; 856–864, 16:
- [10] Ru C, Zhang Y, Sun Y et al. Automated four-point probe measurement of nanowires inside a scanning electron microscope. *IEEE Transactions on Nanotechnology* 2011; 674–681., 10:
- [11] Ye X, Zhang Y, Ru C et al. Automated pick-place of silicon nanowires. *IEEE Transactions on Automation Science and Engineering* 2013; 554–561, 10:
- [12] Zhang Y, Liu XY, Ru CH et al. Piezoresistivity Characterization of Synthetic Silicon Nanowires Using a MEMS Device. *Journal of Microelectromechanical Systems* 2011; 959–967, 20:
- [13] Xie, H., and Régnier, S. (2012). High-efficiency automated nanomanipulation with parallel imaging/manipulation force microscopy. *IEEE Transactions on Nanotechnology*, 11(1), 21-33.
- [14] Rabenorosoa, K., Clévy, C., Lutz, P., Bargiel, S., and Gorecki, C. (2009, November). A micro-assembly station used for 3D reconfigurable hybrid MOEMS assembly-(Special Award). In *IEEE International Symposium on Assembly and Manufacturing*. (Vol. 1, pp. 95-100).
- [15] Courjal N., Caspar A., Eustache C., Behague F., Suarez M. A., Salut R., Rauch J.-Y., Lehmann O., Calero Vila V., Clévy C., Lutz P. and Bernal-Artajona M.-P., Photonic microsystem made by dynamic micro-assembly, in *The International Symposium on Optomechatronic Technology*, Cancun, Mexico, Nov. 2018
- [16] Khalil, W., et Kleinfinger, J. (1986), A new geometric notation for open and closed-loop robots, *Proceedings of the IEEE International Conference on Robotics and Automation*, volume 3, pages 1174–1179.